Comparative Fourier Transform Infrared Studies of the Secondary Structure and the CO Heme Ligand Environment in Cytochrome P-450cam and Cytochrome P-420cam†

Corinne Mouro,‡,§ Christiane Jung,*,‡ Arnaud Bondon,§ and Gérard Simonneaux§

Max Delbrück Center for Molecular Medicine Berlin-Buch, Robert-Rössle-Strasse 10, D-13125 Berlin, Germany, and Laboratoire de Chimie Organométallique et Biologique, UMR 6509, Université de Rennes I, Campus de Beaulieu, F-35042 Rennes Cedex, France

Received January 2, 1997; Revised Manuscript Received April 22, 1997⊗

ABSTRACT: For the first time, Fourier transform infrared spectroscopy has been applied to cytochrome P-450 to analyze the protein secondary structure. From Fourier self-deconvolution and fitting the infrared spectra in the amide I′ region (1600−1700 cm^{-1}), we estimate 44% α-helix, 31% β-sheet, and 18% turns for substrate-free cytochrome P-450cam. In the presence of camphor, 54% α-helix and 3_{10}-helix, 21% β-sheet, and 21% turns are obtained which agree with the crystallographic data of 53% α-helix, 19% β-sheet, and 16% turns [Poulos, T. L., Finzel, B. C., & Howard, A. J. (1987) *J. Mol. Biol. 195*, 687−700]. Cytochrome P-420cam is produced from substrate-free cytochrome P-450cam in two ways: (i) by temperature elevation up to 60 °C and (ii) by exposure to KSCN up to 1.5 M. The secondary structure composition is determined for each temperature and KSCN concentration and compared with the changes observed in the iron ligand CO stretch vibration bands appearing between 1900 and 2000 cm^{-1}. Thermally induced cytochrome P-420 has an α-helix content of 19%, a β-sheet content of 53%, 14% turns, and 5% antiparallel β-sheets from intermolecular hydrogen bonds within protein aggregates. The formation of cytochrome P-420 as a function of the KSCN concentration indicates two types of cytochrome P-420. Up to 1 M KSCN, the induced cytochrome P-420 displays only little modification of the secondary structure, whereas at 1.5 M KSCN, larger changes are observed, resulting in 85% cytochrome P-420 without protein precipitation and containing 30% α-helix, 48% β-sheet, and 17% turns. Infrared spectra in the iron ligand CO stretch region show several subconformers for cytochrome P-420. During the cytochrome P-420 formation, the CO stretch modes are shifted to higher frequencies by 3−11 cm^{-1}, with a main feature at about 1964 cm^{-1}, compared to those of substrate-free cytochrome P-450cam−CO.

Cytochromes P-450 are enzymes which catalyze the hydroxylation of organic compounds implicated in many physiological processes (Schenkman et al., 1993). In this large family, the hemoprotein P-450cam[1] obtained from *Pseudomonas putida* has been widely studied thanks to a series of physical, chemical, and genetic methodologies (Gunsalus & Sligar, 1978; Griffin et al., 1979; White & Coon, 1980; Ortiz de Montellano, 1986; Dawson & Sono, 1987; Sligar et al., 1991). Among these techniques, the X-ray crystallographic investigations of the camphor-bound cytochrome P-450cam have greatly improved the knowledge of the active site (Poulos et al., 1987). The unusual heme axial fifth ligand, a thiolate derived from an endogenous cysteine residue, present in all the P-450 species, gives rise to particular physical characteristics that have been analyzed by a number of spectroscopic methods, as for example optical (Gunsalus et al., 1978), EPR (Lipscomb et al., 1980), resonance Raman (Champion et al., 1978; Ozaki et al., 1978), infrared (O'Keefe et al., 1978; Jung et al., 1992), and NMR spectroscopy (Keller et al., 1972; Philson et al., 1979; Banci et al., 1994). All these analyses improved the knowledge about the protein and permitted the definition of parameters which influence the efficiency of P-450 catalysis.

An undeniable parameter that can strongly deprive the enzyme of its catalytic property is its inactivation through the species commonly called cytochrome P-420. This protein, in the reduced carbon monoxide state, is characterized by its heme absorption at 420 nm, a common optical behavior for the hemoglobin family having a histidine as the fifth ligand of the heme iron. Cytochrome P-420 can be produced by different methods, including temperature or pressure increases, (Hui Bon Hoa et al., 1989; Martinis et al., 1996) and exposure to neutral salts (Imai & Sato, 1967), detergents (Omura & Sato, 1964), organic solvents (Yu & Gunsalus, 1974), or to very low- and high-pH buffer (O'Keefe et al., 1978). In each case, conformational changes in the protein and/or directly in the environment of the iron fifth ligand, resulting in its partial or complete disruption and replacement by a weaker ligand like histidine or methionine (Stern et al., 1973), were suggested. In order to analyze the extent of the secondary structure modifications

† This study was supported in part by the Robert Schuman Foundation Paris, by the European Commission (BIO2-CT94-2060), and by the Deutsche Forschungsgemeinschaft (Ju229/3-1).

* Author to whom correspondence should be addressed. Telephone: 49-30-94063370. Fax: 49-30-94063329. E-mail: cjung@mdc-berlin.de.

‡ Max Delbrück Center for Molecular Medicine Berlin-Buch.

§ Université de Rennes I.

⊗ Abstract published in *Advance ACS Abstracts,* June 1, 1997.

[1] Abbreviations: P-450cam, cytochrome P-450cam, soluble hemoprotein from *Pseudomonas putida* that catalyzes the hydroxylation of (1*R*)-camphor when utilized as the sole carbon source (EC 1.14.15.1, CYP 101; Nelson et al., 1993; FT-IR, Fourier transform infrared; KSCN, potassium thiocyanate.

S0006-2960(97)00017-2 CCC: $14.00

associated with the P-420 formation, we investigated P-450cam and P-420cam using Fourier transform infrared spectroscopy. This is the first FT-IR analysis of the secondary structure of P-450 and P-420 published so far.

The FT-IR technique is a useful method for determining the secondary structure of globular proteins in aqueous solutions. The signals in the different spectral regions are related to the secondary structure (Krimm & Bandekar, 1986). Of all the amide modes of the peptide group, the amide I band is usually taken as being representative of the secondary structure (Miyazawa et al., 1956, 1960; Byler & Susi, 1986). This vibrational mode localized in the spectral region between 1600 and 1700 cm^{-1} originates predominantly from the C═O stretching vibration of the amide group. The amide I contours (amide I′ in deuterated solutions) consist of many overlapping component bands which represent different structural elements such as α-helices, β-sheets, turns, and unordered structures (Susi & Byler, 1986; Byler & Susi, 1986; Krimm & Bandekar, 1986; Surewicz & Mantsch, 1988). The assignment has been established according to the difference in the strength of the hydrogen bonds to the peptide CO group. In addition, the FT-IR technique is an adequate tool for studying the stretching modes of the iron-bound CO ligand in the reduced carbon monoxide−cytochrome P-450cam complex. It has been shown that these stretching modes are an appropriate spectroscopic probe for the heme environment (Jung & Marlow, 1987; Jung et al., 1992, 1996a,b). The overlapping component bands of the CO stretching modes represent different subconformations of the active site. Thus, the FT-IR technique allows the simultaneous study of local changes in the heme pocket as well as global changes in the protein structure. Therefore, this method gives detailed information about the structural behavior of the protein in solution which is not available by the crystal structure data. In particular for cytochrome P-450, which is too large for a complete assignment of the protein protons using the NMR technique, FT-IR spectroscopy is the best method for the mentioned purpose so far.

In this paper, we compare the substrate-free cytochrome P-450cam with the inactive form, cytochrome P-420cam, with regard to their secondary structure and simultaneously the structure of the heme pocket, using the FT-IR method. We investigated two kinds of conversion of P-450 to P-420. One consists of the thermal unfolding of the protein, and the other one uses a neutral salt, the potassium thiocyanate, known to produce quantitatively cytochrome P-420 (Imai & Sato, 1967). The secondary structure estimation for camphor-bound and substrate-free P-450cam in D_2O solution is also compared with the results of the crystal structure analysis.

MATERIALS AND METHODS

Cytochrome P-450cam (CYP101) is expressed in *Escherichia coli* TB1 cells and purified to an absorbance ratio (392 nm/280 nm) of 1.4 as previously described (Jung et al., 1992). Camphor is removed according to the method described by Poulos and Wagner (1982). The protein is first dialyzed against 100 mM Tris-HCl buffer at pH 7 and loaded onto a Sephadex G25 column equilibrated with the same buffer. The pure substrate-free P-450cam is then concentrated to a final concentration of about 1 mM and extensively dialyzed against 100 mM D_2O phosphate buffer at pH 7 in a water vapor-tight glovebox.

For the experiments using the potassium thiocyanate, a 12.5 M stock solution of KSCN in deuterated phosphate buffer is prepared and stored at 4 °C.

The SCN^- dissociation constant K_d is determined in titration experiments followed in the absorbance change of the Soret band of oxidized P-450. The P-450 concentration for these experiments is 18 μM. At each titration step, the spectrum of the carbon monoxide complex is checked for P-420 formation. It revealed that P-420 formation requires a long KSCN incubation time of 10 h at 4 °C.

For the infrared spectroscopic studies, three solutions of 0.4 mM substrate-free P-450cam containing KSCN at different concentrations (0.5, 1, and 1.5 M) are stored at 4 °C over the course of 10 h.

The carbon monoxide complex of P-450cam is prepared in the following way. Forty microliters of a 0.4 mM protein solution (previously prepared by dilution of a 1 mM stock solution or for the KSCN experiments, according to the added volume of potassium thiocyanate) is saturated with CO by passing a strong gas stream over the surface of the stirred solution for 1 min. A total of 3 μL of a 1 M sodium dithionite solution (in the deuterated phosphate buffer) is added, and the reduced protein is flushed with CO for a further 1 min.

The sample is immediately loaded into the infrared cell, installed in a cell holder thermostated at 4 °C, and checked in the electronic absorption spectrophotometer (Shimadzu 2101PC) for the P-420 conversion. The concentration of P-450cam (0.4 mM) is calculated using an absorption coefficient at 446 nm of 127 mM^{-1} cm^{-1} (Gunsalus & Sligar, 1978). The protein concentration of 0.4 mM is found to be optimal for resolving simultaneously the amide bands and the stretch vibration mode of the CO iron ligand which have approximately 100-fold less absorbance than the amide I′ band.

Infrared spectra are recorded using the Bruker IFS 66 Fourier transform infrared spectrometer equipped with a liquid nitrogen-cooled MCT detector. The protein solution is placed in a homemade demountable cell with CaF_2 windows and a 65 μm Teflon spacer. To compensate for the deuterated buffer absorption, a buffer solution is placed in the same cell and the spectrum is measured using the same temperature and measurement parameters.

The samples are thermostated using the Peltier-type TSK 200 thermostat (Wissenschaflicher Gerätebau, Berlin).

The resolution is set to 2 cm^{-1} with a double-sided/forward−backward acquisition mode. Fourier transformation of 200 co-added interferograms is performed with the Blackman-Harris four-term apodization function and a zero-filling factor of 2.

The protein spectra are obtained by substracting the deuterated buffer spectrum from the individual spectra of the protein measured at the same temperature.

In order to eliminate spectral contributions due to the atmospheric water vapor, the instrument is continuously purged with dry air. In addition, a water vapor spectrum is recorded under similar conditions using the same instrumental parameters as those used for the protein sample. The water vapor spectrum is then interactively substracted from the buffer-corrected spectrum of the protein until a flat baseline between 1715 and 1745 cm^{-1} is obtained.

Spectra in the presence of potassium thiocyanate show a strong absorption at about 2064 cm^{-1}. An interactive

substraction of the KSCN spectrum from the sample spectrum is performed between 2000 and 1900 cm^{-1} until a sufficiently flat baseline is obtained for analyis of the CO ligand stretching modes.

Some amino acid side chain groups absorb in the amide I′ spectral region of proteins (Chirgadze et al., 1975). To obtain the pure peptide absorption, an accurate substraction of the side chain absorptions is necessary.

Absorption spectra from the side chains of tyrosine, arginine, glutamine, asparagine, and aspartic and glutamic acids are rebuilt from the numerical values of the molar extinction coefficients (ϵ_k) of these residues' side chains, estimated by Chirgadze et al. (1975), in a D_2O solution between 1500 and 1800 cm^{-1}.

The following equation is used to calculate the absorption spectrum of the side chains:

$$A(\nu) = \epsilon(\nu)[\mathrm{P}]S$$

with

$$\epsilon(\nu) = \sum n_k \epsilon_k(\nu)$$

where $A(\nu)$ and $\epsilon(\nu)$ are the absorbance and the molar absorption coefficient of the global side chain band, respectivley, n_k is the number of k residues in the protein, $\epsilon_k(\nu)$ is the molar extinction coefficient at frequency ν of residue k, [P] is the protein concentration (0.4 mM), and S is the size of the path length (65 μm). The number of the amino acids considered are taken from the crystal structure (Poulos et al., 1987): Tyr (9), Arg (26), Gln (23), Asn (13), Asp (22), and Glu (33).

Resolution enhancement of the spectra is carried out with the Bruker software. The second derivative is applied to the original spectra in the amide I′ region with a 13-point smoothing function. Deconvolution is performed by using Lorentzians, a deconvolution factor of 5000 (corresponding to a Lorentz half-bandwidth of 16 cm^{-1}), and a noise reduction factor of 0.3. A baseline correction using the Bruker software (Bezier function) is made on each side of the deconvoluted amide I′ band.

The baseline for the spectra of the stretching modes of the CO ligand bound to the iron is corrected by fitting the right and the left side of the spectra where no CO stretching modes appear (1913−1923 and 1986−1996 cm^{-1}) using a cubic polynomial function with a least-square fit procedure (O. Ristau, unpublished program).

Curve fitting of the baseline-corrected deconvoluted amide I′ spectra and of the corrected CO stretching mode spectra is performed using a nonlinear least-squares curve-fit procedure using the Gauss line shape profile.

The number of bands and their position for fitting the amide I′ spectra are taken from the second-derivative spectra. For the CO iron ligand spectra, we used a model which considers the minimal number of bands necessary to fit the spectra sufficiently well as we have previously published (Jung et al., 1996a).

The percentage amount of the different secondary structure elements is estimated from the relative area of the corresponding bands. The percentage of P-420 formation is calculated from the absorbance increase of the Soret band in the carbon monoxide complex at 420 nm relative to the maximal absorbance for pure P-420.

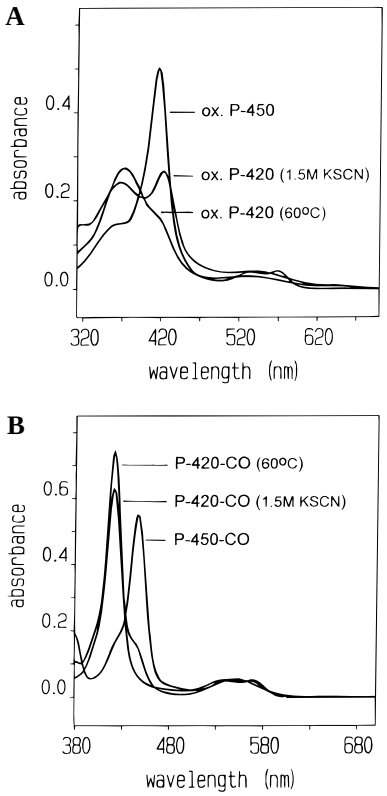

FIGURE 1: Electronic absorption spectra of the substrate-free cytochrome P-450cam, thermally induced cytochrome P-420 (60 °C), and chemically induced cytochrome P-420 (1.5 M KSCN) in their oxidized state (A) and their carbon monoxide-reduced state (B). Spectra measured in the IR cells (65 μm spacer) in 0.1 M potassium phosphate buffer at pH 7.

RESULTS AND DISCUSSION

The conversion of substrate-free P-450cam to the inactive form, P-420, is induced using two methods: (i) by heating the protein to 60 °C for 10 min and (ii) by addition of high concentrations of KSCN and storing the samples at 4 °C over the course of 10 h. Analysis of the electronic absorption spectra permits first checking of the P-420 formation. Then, more precise FT-IR studies are carried out in the amide I′ spectral region and simultaneously in the CO iron ligand part. Thus, the active form and the inactive form thermally and chemically induced are compared with regard to their secondary structure and the conformations of their heme pocket.

Electronic Absorption Spectra. The optical spectrum of the oxidized substrate-free P-450cam shows a Soret band at 417 nm with a shoulder at 360 nm and the α- and β-bands at 568 and 534 nm, respectively (Figure 1A). This spectrum defines the low-spin state of P-450cam (Rein et al., 1984). In its carbon monoxide complex, the Soret band is at 446 nm and the Q band at 553 nm, typically observed if a cysteinate functions as the fifth ligand of the iron (Figure 1B).

Substrate-free P-450cam is efficiently converted to P-420 by heating the protein at 60 °C for 10 min or after its exposure to 1.5 M KSCN at 4 °C for 10 h. The optical spectrum of the thermally induced P-420 reveals a Soret band at 370 nm with a shoulder at 419 nm. The former Soret

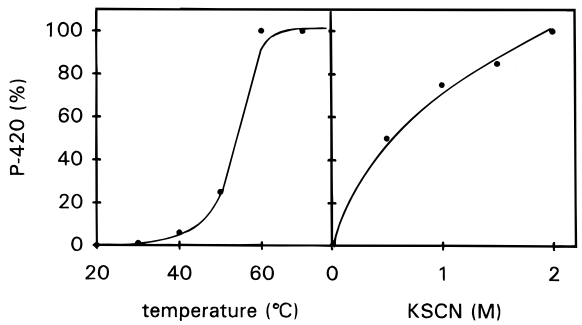

FIGURE 2: P-420 transition curve of the substrate-free cytochrome P-450cam estimated from the Soret band absorbance at 420 nm in the CO complex relative to the maximal absorbance value for complete conversion. Plot as a function of the temperature and of the KSCN concentration.

band has been assigned to the five-coordinate high-spin P-420, and the latter one corresponds to the six-coordinate low-spin P-420 (Wells et al., 1992). The visible bands are located between 530 and 540 nm with a weak band at around 650 nm. The experiments concerning the chemical denaturation with 1.5 M KSCN give an optical spectrum with two peaks in the Soret band region at 422 and 368 nm with almost similar intensities (Figure 1A). A shoulder at 568 nm on the visible band between 530 and 540 nm appears. Reduction of the thermally and chemically induced P-420 by potassium dithionite results in a Soret band at 424−425 nm and visible bands at 530 and 558−559 nm. After a strong stream of carbon monoxide gas was passed over the surface of the stirred P-420 solution, the characteristic bands at 420, 538−539, and 568−569 nm are observed (Figure 1B).

The different Soret band found for the oxidized state of chemically generated P-420 as compared to that of the thermally induced one originates from the binding of thiocyanate to the heme iron as previously reported for P-450 by Dawson et al. (1992). We tried to verify the binding of SCN^- to the heme iron by infrared experiments. Unfortunately, in the relevant infrared spectral region, we could not detect any separate signal which might correspond to a stretch vibration of SCN^- bound to the heme iron. We see only the intense band of free KSCN around 2064 cm^{-1}. Scheidt et al. (1982) reported that the SCN^- stretch vibration shifts only by 10 cm^{-1} to lower frequencies during binding to an iron(III) complex which led us to expect that we cannot separate the stretch vibration bands for the free and iron-bound SCN^-.

Figure 2 shows the transition amount to P-420 as a function of the temperature and for various KSCN concentrations. At 50 °C, only around 25% of substrate-free P-450cam is converted to the inactive form. The complete denaturation occurs at 60 °C (Figure 2). The plot of the P-420 content versus the temperature follows a strongly asymmetric S shape with a half-transition temperature $T_{1/2}$ around 54 °C. The substrate-free P-450cam is more stable in deuterated phosphate buffer than in the protonic water. The optical half-transition temperature $T_{1/2}$ found in protonic buffer is around 40 °C (Jung et al., 1985). An increased thermal stability in deuterated buffer has also been observed for other proteins (Harrington & Hippel, 1961) and seems to be a general phenomenon. Scanning calorimetric studies (Jung et al., 1985; Pfeil et al., 1993) and a search for hydrophilic intramolecular interfaces in the three-dimensional

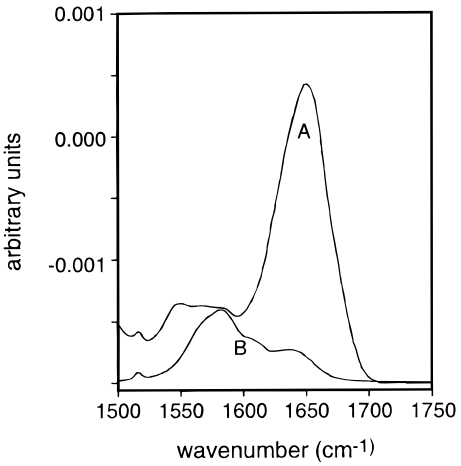

FIGURE 3: Original infrared spectrum of substrate-free cytochrome P-450cam at 20 °C in the spectral region of the amide I′ and amide II bands. Spectra measured in D_2O potassium phosphate buffer (A). Amino acid side chain group absorption band calculated for cytochrome P-450cam in D_2O potassium phosphate buffer according to its amino acid composition (see Materials and Methods) (B).

crystal structure revealed three domains and three cooperative unfolding units with transition temperatures at around 42 °C (unit 1, loosening of interactions between the three domains), 48 °C (unit 2, unfolding of domain 2), and 54 °C (unit 3, unfolding of domains 1 and 3) (Jung et al., 1994). Because of the stabilizing effect of D_2O, unfolding units 1 and 2 seem to be shifted to higher temperatures.

KSCN titration experiments yield a dissociation constant K_d of 25 mM which is in agreement with the value of 26 mM already reported earlier by Sono et al. (1982). Figure 2 (right side) shows the P-420 formation as a function of the KSCN concentration. P-420 at 100% is observed with 2 M KSCN but is accompanied by strong aggregation and precipitation of the protein. It is important to note that 10 h is required for the P-420 formation in the presence of KSCN independent of the P-450 concentration used. This long incubation time required might indicate that KSCN has to penetrate the protein structure to induce structural changes. The KSCN access into the protein might be kinetically hindered because of the insufficiency of protein fluctuations.

FT-IR Spectra of P-450cam and P-420cam and Secondary Structure Estimation. Figure 3 shows the Fourier transform infrared amide I′ spectrum of substrate-free P-450cam and the calculated amino acid side chain absorption spectrum in the 1500−1800 cm^{-1} region. This side chain spectrum has been subtracted from the spectrum of the P-450 and P-420 spectra before further analysis by deconvolution and fitting. The amide I′ band is centered at around 1650 cm^{-1}, which is characteristic for a protein rich in α-helix content (Byler & Susi, 1986). Resolution enhancement through Fourier self-deconvolution facilitates the curve fitting analysis.

Figure 4A shows the fitted deconvoluted amide I′ band of the camphor-bound P-450cam at 20 °C. Ten bands at 1600, 1611, 1622, 1632, 1641, 1649, 1658, 1666, 1673, and 1689 cm^{-1} are obtained. All band parameters were varied during the fitting. Different start values for the band parameters give the same results. Table 1 summarizes the position and population of the bands and their designation to structural elements according to the assignment of the individual bands to secondary structure elements from published FT-IR data of many other proteins (Susi & Byler,

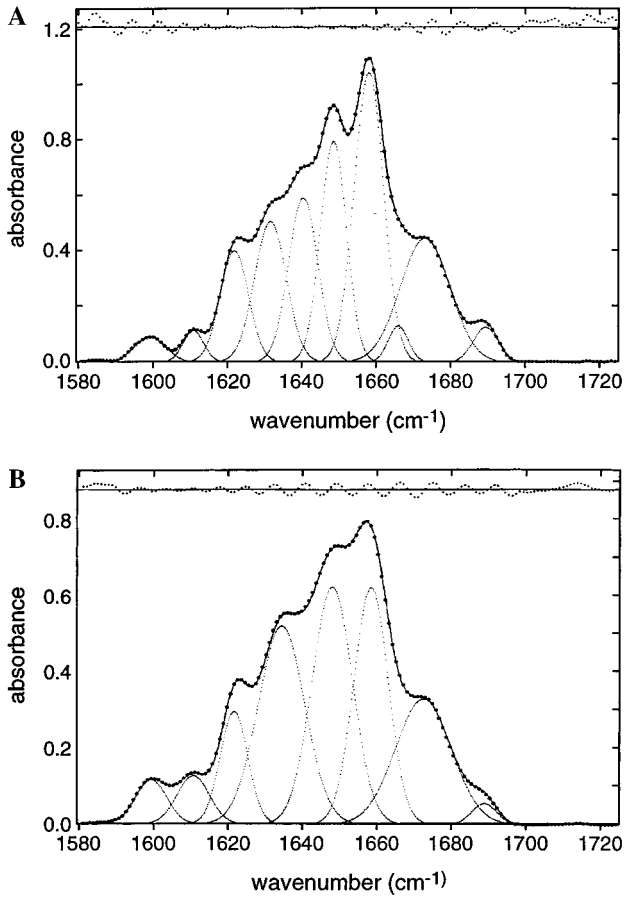

FIGURE 4: Fitted self-deconvoluted amide I′ bands of the substrate-bound cytochrome P-450cam at 20 °C (A) and the substrate-free cytochrome P-450cam at 20 °C (B). Experimental spectra (●), individual Gaussian components (•••), the sum spectrum (---), and residuals (top).

Table 1: Amide I′ Component Bands, Relative Integrated Intensities (Population), and Secondary Structure Assignments for Camphor-Bound and Substrate-Free Cytochrome P-450cam in D_2O Phosphate Buffer

camphor-bound		substrate-free		
position (cm^{-1})	population (%)	position (cm^{-1})	population (%)	assignment
1599.6 ± 0.1	2	1599.5 ± 0.1	3	Arg side chain
1611.1 ± 0.1	2	1610.8 ± 0.1	4	Arg, Tyr side chain
1622.1 ± 0.2	9	1621.8 ± 0.1	8	β-sheets
1631.8 ± 0.3	12	1634.6 ± 0.2	23	β-sheets
1640.7 ± 0.2	14	−	−	α-helix,3_{10}-helix
1648.8 ± 0.1	16	1648.2 ± 0.1	24	α-helix
1658.2 ± 0.1	24	1658.6 ± 0.1	20	α-helix
1666.1 ± 0.1	2	−		turns
1673.2 ± 0.1	17	1672.5 ± 0.1	17	turns
1689.3 ± 0.1	2	1688.7 ± 0.1	1	turns

1986; Byler & Susi, 1986; Krimm & Bandekar, 1986; Surewicz & Mantsch, 1988; Arrondo et al., 1988; Prestrelski et al., 1991). The features at 1649 and 1658 cm^{-1} are assigned to the α-helix structure. A band at 1641 cm^{-1} is often connected with unordered structures, but its high intensity in P-450 and its position nearby α-helix components might suggest that it contains α-helix-type structures as extended chains connecting the helical cylinders and loops of the α-type (Byler & Susi, 1986). The 3_{10}-helix is also characterized by a band at around 1640 cm^{-1} in D_2O buffer (Holloway et al., 1989) and might correspond to the amino acid sequences 77−81 and 324−328 which have been assigned in the crystal structure as a 3_{10}-helix (Poulos et al., 1987). These three bands represent the 13 helices (A−L) found in the crystal structure. The sum of the integrated intensities of these bands give an α-helix and 3_{10}-helix content of 54% which matches well the value of 53% obtained from the crystal structure. Infrared bands corresponding to β-sheets occur generally in the region between 1620 and 1637 cm^{-1} as strong components and at around 1672 cm^{-1} as a weak component (Byler & Susi, 1986). The P-450 bands at 1622 and 1634 cm^{-1} are assigned as β-sheets β_1 to β_5 seen in the crystal structure. From the integrated intensity, we estimate a β-sheet content of 21% which agrees with the 19% obtained from the crystal structure. The usually observed low-component β-sheet signal at around 1672 cm^{-1} may contribute to the feature seen at 1673 cm^{-1}; however, the relatively strong integral intensity of this band excludes the assignment as pure β-sheet signal. This would overestimate the total β-sheet content. Bands appearing between 1666 and 1690 cm^{-1} are generally assigned to turn structures. Therefore, we assign the features at 1666, 1673, and 1689 cm^{-1} to turns. The integrated intensities of the three bands correspond to 21% which is slightly higher than the 16% seen in the crystal structure. A clear assignment for the bands at 1600 and 1611 cm^{-1} which have a small population of around 4% is not possible. However, it might be that the arginine side chain absorption and/or tyrosine absorption is not completely compensated with the method described above because some of the 26 arginine and/or 9 tyrosine residues may have shifted frequencies compared to the standard spectra taken from Chirgadze et al. (1975).

Figure 4B shows the deconvoluted spectrum with its component bands obtained for substrate-free P-450cam. The spectrum is characterized by eight peaks at 1600, 1611, 1622, 1635, 1648, 1659, 1672, and 1689 cm^{-1} (Table 1). At the first sight, the quantitative examination of the secondary structure of substrate-free P-450cam calculated at room temperature (20 °C) differs slightly from the structural distribution of the camphor-bound P-450cam. The two bands at 1648 and 1658 cm^{-1} in substrate-free P-450 assigned to α-helix total 44% of the structure. The band at 1641 cm^{-1} observed for camphor-bound P-450cam, assigned as (3_{10}-helix and α-helix), is not obtained. The β-sheets represent 31% (1634 and 1622 cm^{-1}). It seems that about 10% of the 3_{10}-helix and α-helix is lost in favor of β-sheets. However, the lower resolution of the spectrum for the substrate-free protein results in an increased width of the band at 1635 cm^{-1} (14.8 compared to 10.0 cm^{-1} for camphor-bound P-450) and a frequency shift of 4 cm^{-1} in the direction of the α-helix bands. This may be indicative of a higher mobility in the protein structure and/or an increase of the number of subconformers (Ismail et al., 1992) due to the absence of camphor. Whether this lower α-helix content reflects the observed higher mobility of residues Phe87−Tyr96, which include the B′-helix, and around Thr185, which is part of a loop connecting two antiparallel helices (F and G) (Poulos et al., 1986), has yet to be verified. The small band at 1666 cm^{-1} observed in camphor-bound P-450cam and assigned to turns is not resolved in the spectrum for the substrate-free protein. However, the band at 1672 cm^{-1} shows a larger width (17.5 compared to 15.5 cm^{-1} for camphor-bound P-450cam) and may therefore cover the feature at 1666 cm^{-1}. Eighteen percent turn structure is estimated from the bands at 1672 and 1689 cm^{-1}.

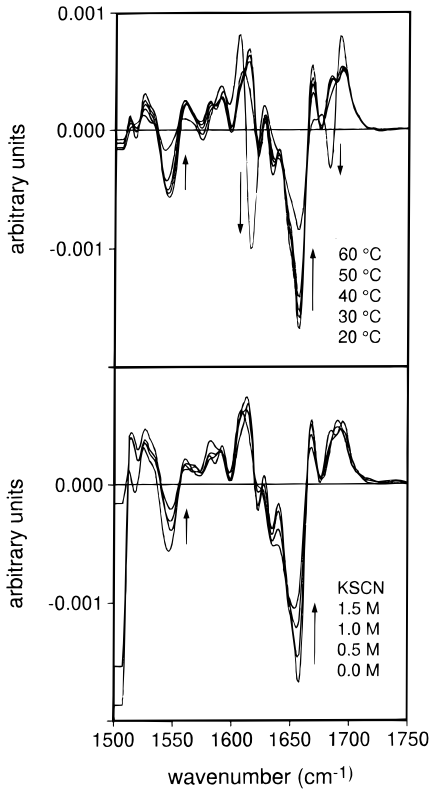

FIGURE 5: Second-derivative spectra of substrate-free cytochrome P-450cam measured in D_2O potassium phosphate buffer as a function of the temperature (top) and of the KSCN concentration (bottom). Second-derivative spectra were obtained from the original absolute spectra after a 13-point smoothing.

Table 2: Amide I′ Component Bands, Relative Integrated Intensities (Population), and Secondary Structure Assignments for Substrate-Free Cytochrome P-420cam in D_2O Phosphate Buffer

thermal (60 °C)		chemical (1.5 M KSCN)		
position (cm^{-1})	population (%)	position (cm^{-1})	population (%)	assignment
1599.6 ± 0.4	3	1599.1 ± 0.1	2	Arg side chain
		1611.2 ± 0.2	1	Arg, Tyr side chain
1614.6 ± 0.8	6	−		antiparallel β-sheets
1618.7 ± 9.2	5	1619.7 ± 0.1	4	β-sheets
1638.7 ± 1.6	48	1636.4 ± 0.8	44	β-sheets
1648.2 ± 0.5	4	1649.8 ± 0.7	16	α-helix
1658.5 ± 0.2	15	1658.5 ± 0.3	14	α-helix
1672.3 ± 0.7	14	1670.1 ± 0.4	14	turns
		1681.1 ± 1.4	3	turns
1684.2 ± 0.1	5	−		antiparallel β-sheets

Changes in the secondary structure occurring during the P-450 to P-420 conversion are best demonstrated in the second-derivative spectrum (Figure 5). At first sight, thermally induced P-420 (60 °C) reveals two new component bands at 1614 and 1684 cm^{-1} arising mainly between 50 and 60 °C. Simultaneously, the band at 1658 cm^{-1} decreases. In the presence of KSCN, a loss of the population of the band at 1658 cm^{-1} is also observed; however, weaker variations of the other peaks are noticed, and no new signal appears.

Fourier self-deconvolution and curve fitting are performed for the spectra at 20, 30, 40, 50, and 60 °C and for KSCN concentrations of 0.5, 1, and 1.5 M (Tables 2 and 3). Panels A and B of Figure 6 show the fitted spectra for P-420cam at 60 °C and 1.5 M KSCN, respectively.

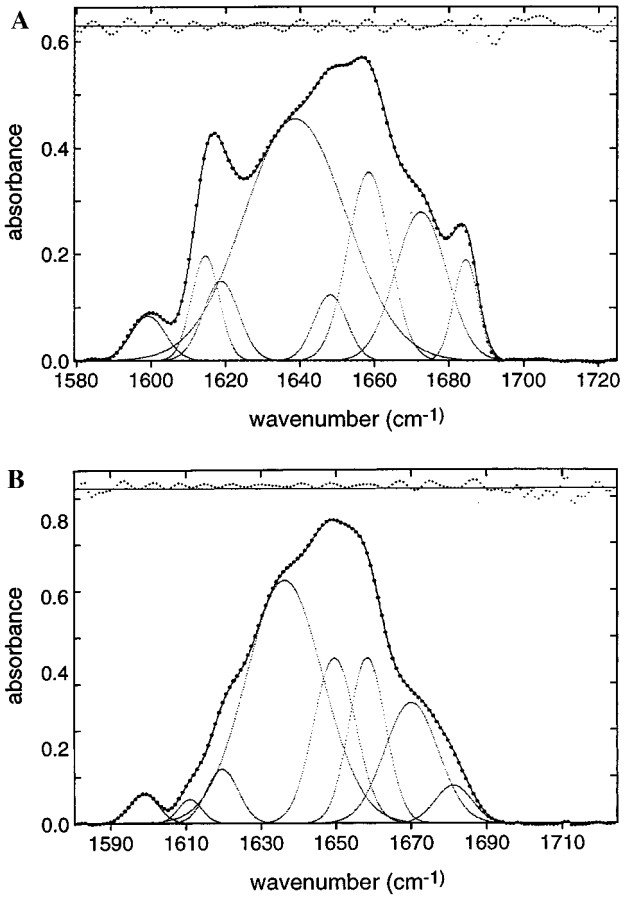

FIGURE 6: Fitted self-deconvoluted amide I′ bands of cytochrome P-420cam thermally induced at 60 °C (A) and chemically induced by 1.5 M KSCN (B). Experimental spectra (●), individual Gaussian components (•••), the sum spectrum (---), and residuals (top).

During the thermal unfolding between 30 and 50 °C, the band at 1648 cm^{-1} assigned to α-helix loses 12% of the population while the component at 1634 cm^{-1} corresponding to β-sheets increases by 10% (Table 3). Smaller alterations are observed for the other bands. In this temperature range, only 25% P-420 is formed, estimated from the Soret band absorbance at 420 nm in the CO complex relative to the maximal absorbance value for the complete conversion. Beyond 50 °C, gel formation is seen to be linked to the appearance of the two new bands at 1614 and 1684 cm^{-1}. These bands have been seen also for other proteins and are assigned to strong intermolecular hydrogen bonding in antiparallel β-sheets (Clark et al., 1981; Carrier et al., 1990; Muga et al., 1990; Ismail et al., 1992). Further heating to 60 °C induces 100% P-420 formation and results then in the unfolded protein with an additional decrease of α-helix character (6% of the 1648 cm^{-1} type, 11% of the 1658 cm^{-1} type), while the β-sheet character increases by an additional 15%. The band at 1634 cm^{-1} becomes very broad, indicating a wide distribution of various β-sheets with different microenvironments. Although the new bands at 1614 and 1684 cm^{-1} are clearly resolved in the deconvoluted spectrum and in the second-derivative spectrum, they contribute only approximately 6 and 5% to the total integrated intensity, respectively. They cannot be differentiated in the fitting from native P-450 bands at 1611 cm^{-1} resulting from residual arginine or tyrosine side chain absorption and those at 1688 cm^{-1} assigned to turns assuming that the contributions of these structures are unchanged during heating. The strong

Table 3: Population (Percent) of the Amide I′ Subbands for Substrate-Free Cytochrome P-450cam−CO Obtained from Curve Fitting of the Deconvoluted Infrared Spectra at Various Temperatures and KSCN Concentrations[a]

band	1600 cm^{-1} band	1611 cm^{-1} band	1614 cm^{-1} band	1622 cm^{-1} band	1634 cm^{-1} band	1648 cm^{-1} band	1658 cm^{-1} band	1672 cm^{-1} band	1681 cm^{-1} band	1684 cm^{-1} band
temperature										
20 °C	3	4	−	8	23	24	20	17	1	−
30 °C	3	2	−	7	23	22	23	18	1	−
40 °C	2	3	−	6	29	16	25	18	1	−
50 °C	2	5	−	4	33	10	26	19	1	−
60 °C	3	−	6	5	48	4	15	14	−	5
KSCN										
0.0 M	3	4	−	8	23	24	20	17	1	−
0.5 M	2	1	−	8	22	30	18	18	1	−
1.0 M	2	1	−	7	26	31	12	19	2	−
1.5 M	2	1	−	4	44	16	14	15	3	−

[a] The bands are assigned by their approximate frequency values. Detailed fit data and assignment to secondary structure elements are given in Table 2.

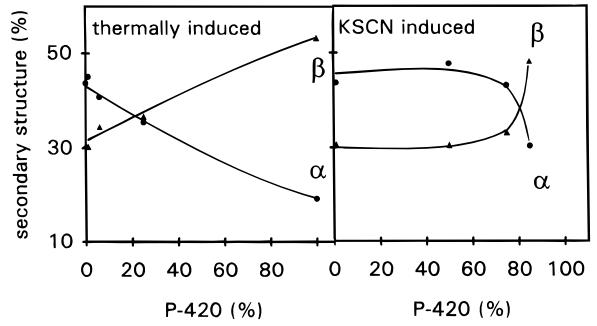

FIGURE 7: Correlation between the P-420 amount and the secondary structure element content for thermally induced and KSCN-induced conversion.

decrease of the intensity of the amide II band centered at around 1545 cm^{-1} starting at 50 °C (Figure 5) indicates unfolding of the protein core with exposure of interior protons to the solvent. The amide II band, originated from coupled C−N stretching and N−H bending modes which appears in protonic water between 1540 and 1550 cm^{-1}, is shifted to 1458 cm^{-1} in D_2O (C−N stretching and N−D bending) (Wong, 1991). Even after extensive dialysis against D_2O buffer, a band at 1540 cm^{-1} is observed in P-450cam originating from interior N−H bonds which cannot be exchanged to N−D. At about 50 °C, these interior N−H groups are accessible to the solvent. This phenomenon is a good probe of the polypeptide unfolding and has been observed in many other proteins in this temperature region (Ismail et al., 1992; Van Stokkum et al., 1995; Holzbaur et al., 1996). Comparing the spectra at 20 and 60 °C, we can conclude that the main structural change during the P-450 to P-420 conversion is a decrease of the α-helix content by 25% and an increase of the β-sheet content by 22%, while additionally, 4% of turns are lost and 5−6% of new structures generally defined as antiparallel β-sheets with the appearance of strong intermolecular hydrogen bonding. The α-helix content matches the value of approximately 20% which we have recently determined using circular dichroism measurements at 70 °C for the thermal unfolding of oxidized P-450cam in protonic phosphate buffer solution in the presence and in the absence of camphor (Nölting et al., 1992). Figure 7 demonstrates that the loss of the total α-helix content and the increase of the total β-sheet content correlate linearily with the amount of P-420 formed while heating.

Exposure of the protein to 0.5 M KSCN over the course of 10 h at 4 °C produces 51% P-420 estimated from the Soret band in the carbon monoxide complex. The formation of this large amount of P-420 is however accompanied only by small changes in the secondary structure (Table 3). In the presence of 1 M KSCN, 77% P-420 is formed and the main effect is the conversion of approximately 4% α-helix of the 1658 cm^{-1} type to β-sheet of the 1634 cm^{-1} type. For 1.5 M KSCN, 14% of the α-helix content is converted to extended chains and/or β-sheets of the 1634 cm^{-1} type. A P-420 content of 85% is obtained. In contrast to thermal denaturation, no aggregation or precipitation appears at this high KSCN concentration. The sample solution remains clear, and the typical bands for hydrogen bonding in intermolecular antiparallel β-sheets are not observed. The bands at 1681 and 1611 cm^{-1} can therefore not be assigned to a possibly weakened intermolecular β-sheet hydrogen bonding in the presence of KSCN. In summary, Figure 7 shows that the relation between the KSCN-induced changes in the secondary structure and the P-420 formation is qualitatively different from the thermally induced conversion.

Changes in the Heme Pocket and Its Relation to Alterations in the Secondary Structure. Panels A−C of Figure 8 show the fitted baseline-corrected infrared spectra for the CO stretching modes of the substrate-free P-450cam and the thermally and chemically induced P-420cam. The spectrum for the substrate-free P-450cam (Figure 8A) shows two peaks at around 1940 and 1963 cm^{-1} which have to be decomposed as a minimal fit model by five Gaussian bands centered at about 1934 (band II), 1941 (band III), 1954 (band IV), 1963 (band V), and 1973 cm^{-1} (band VI). This classification follows results previously obtained by Jung et al. (1996a). Concerning the minor band at 1973 cm^{-1}, it is difficult to say whether this component originates from the baseline correction or whether it represents a real conformation as already discussed by Jung et al. (1996a). The P-420 heme pocket is also characterized by several subconformations since four or five CO stretching modes are observed (Figure 8B,C). We use the same nomenclature of the bands (II−VI) for P-450 because systematic shifts to the blue spectral region are observed during the P-420 formation. Moreover, for KSCN concentrations beyond 1 M, we cannot distinguish between bands V and VI. The curve fitting gives only one Gaussian around 1975 cm^{-1}, while a second Gaussian assumed for band V or VI is always shifted outside the spectral region of the CO stretch modes. Table 4 summarizes the fit results.

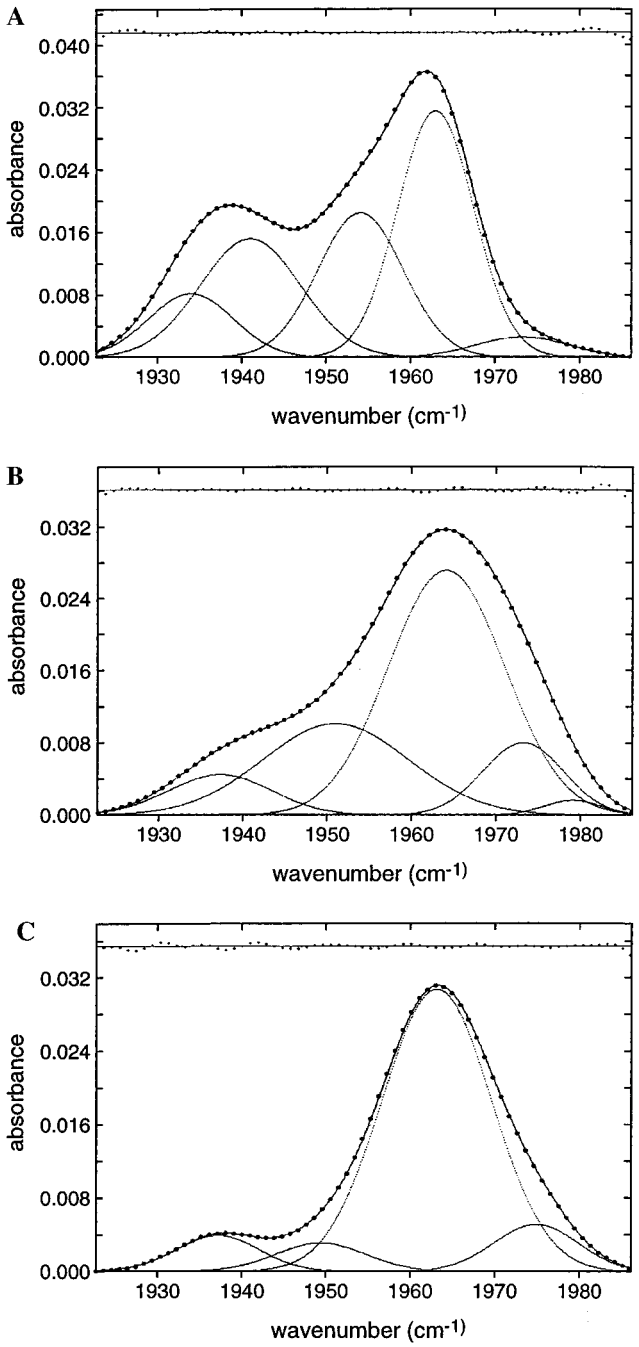

FIGURE 8: Fitted infrared spectra for the carbon monoxide ligand stretching modes of the substrate-free cytochrome P-450cam at 20 °C (A), the thermally induced cytochrome P-420 at 60 °C (B), and the chemically induced P-420 (1.5 M KSCN) (C). Experimental spectra (●), individual Gaussian components (···), their sum (---), and residuals.

Warming substrate-free P-450cam from 20 to 50 °C does not significantly change the CO stretch wavenumber of the bands except that of band IV which shows a blue shift of 5 cm^{-1} (Figure 8A). However, a population exchange from substate V to IV is observed to be the main effect. Bands IV and V have been shown to result from a less tight polar contact of the CO ligand to the Thr252 region compared to that to substate III due to influx of water into the protein structure (Jung et al., 1996a). Obviously, these subconformations are less stable against temperature elevation and may be therefore more accessible to P-420 formation. These changes may be correlated to the 12% loss of α-helix content and the formation of 25% P-420. In contrast, the lower-frequency modes representing subconformations II and III, which have been shown to possess a stronger polar contact to the I-helix, are less influenced in this temperature range (20−50 °C), indicating a higher thermal stability.

In the narrow temperature range between 50 and 60 °C, 75% of the protein is converted to P-420. Stretching mode bands II, III, and V of the CO ligand become broader by 3−7 cm^{-1} except for band IV which has a smaller width by 5 cm^{-1}. The frequency of all bands is strongly blue shifted by 3−11 cm^{-1} (Table 4). A population exchange is observed from component IV to III and V. The increase in the band width may be indicative of a higher number of subconformers (Ismail et al., 1992). These changes correlate with the additional loss of 17% of α-helix content and the broad band at 1635 cm^{-1} representing the increase of 15% of β-sheet structure. The strong blue shift of all bands indicates important changes in the polarity of the distal side (Jung et al., 1996a,b) and/or in the fifth ligand region. Quantum chemical calculations for porphyrin iron−CO complexes (Jung, 1983, 1985) suggest that the general blue shift could originate from the protonation of the cysteinate or from its substitution by imidazole of a histidine. Another explanation is related to the electronic resonance structure of the Fe−CO group and its possible stabilization by positive or negative electrostatic potentials on the distal side (Li et al., 1994). Indeed, recently, we have shown that a higher content of water in the heme environment could result in the compensation of a supposed positive electrostatic potential near the CO ligand which would result in loosening of the contact of CO to the I-helix. This causes the increase of the CO stretch vibration wavenumber (Jung et al., 1996b) as it is also observed for the thermally induced P-420. From our experiments, however, we cannot differentiate between these two interpretations.

The KSCN-induced changes in the CO stretch mode spectrum differ from the thermally caused alterations. Exposure of substrate-free P-450cam to 0.5 M KSCN at 4 °C over the course of 10 h induces no remarkable changes in the secondary structure, but a P-420 conversion rate of 51% is observed. In this concentration range, the wavenumbers of CO stretch bands II−VI are almost unchanged. However, a strong population transfer is observed from subconformations III and V to IV. Increasing the KSCN concentration to 1 M induces the increase of the P-420 content to a value of 77%. All CO stretch bands show a blue shift of approximately 5−12 cm^{-1}, indicating strong changes in the heme pocket structure. Subconformations V and VI lose population in favor of subconformations IV and II compared to that with 0.5 M KSCN. These changes are accompanied by the conversion of approximately 4% α-helix of the 1658 cm^{-1} type to β-sheet of the 1634 cm^{-1} type. At 1.5 M KSCN, the wavenumber of the CO stretch bands remains unchanged compared to that with 1 M KSCN. Subconformation IV is however additionally populated by 13%, while subconformations II and III lose population by 10 and 5%, respectively. A final P-420 content of 85% is obtained. In the concentration range of 1−1.5 M KSCN, the main change in the secondary structure is observed as discussed above.

The thermally and chemically induced changes observed in the CO stretch bands are very complex. We tried to correlate quantitatively the parameters obtained from fitting the CO stretch spectra with the percentage of secondary

Table 4: Frequency and Population of the CO Iron Ligand Subbands for Substrate-Free Cytochrome P-450cam−CO Obtained from Curve Fitting of the CO Stretch Infrared Spectra at Various Temperatures and KSCN Concentrations[a]

band	band II (cm^{-1}) (%)	band III (cm^{-1}) (%)	band IV (cm^{-1}) (%)	band V (cm^{-1}) (%)	band VI (cm^{-1}) (%)
temperature					
20 °C	1933.9 ± 0.1	1940.9 ± 0.2	1954.2 ± 0.8	1963.5 ± 0.3	1972.8 ± 0.2
	11	24	25	37	3
30 °C	1931.7 ± 0.8	1938.8 ± 0.5	1957.5 ± 0.2	1963.5 ± 0.3	1972.8 ± 0.2
	5	22	58	14	1
40 °C	1933.1 ± 6.9	1940.1 ± 0.1	1957.7 ± 9.2	1962.9 ± 0.1	1976.3 ± 1.0
	7	20	59	13	1
50 °C	1933.8 ± 6.2	1940.6 ± 0.1	1959.5 ± 0.1	1962.2 ± 8.0	1977.6 ± 0.2
	6	17	67	8	2
60 °C	1937.2 ± 0.1	1950.9 ± 0.1	1964.1 ± 0.5	1973.1 ± 0.1	1978.9 ± 0.1
	8	26	54	11	1
KSCN					
0.0 M	1933.9 ± 0.1	1940.9 ± 0.2	1954.2 ± 0.8	1963.5 ± 0.3	1972.8 ± 0.2
	11	24	25	37	3
0.5 M	1933.1 ± 0.1	1939.3 ± 0.1	1955.0 ± 2.1	1963.7 ± 0.1	1976.0 ± 4.0
	10	10	46	29	5
1.0 M	1937.1 ± 0.1	1951.7 ± 0.8	1963.3 ± 0.1	1975.9 ± 0.2	1975.9 ± 0.2
	17	11	64	8	−
1.5 M	1937.0 ± 0.2	1949.5 ± 0.2	1963.2 ± 0.1	1974.9 ± 0.2	1974.9 ± 0.2
	7	6	77	10	−

[a] Assignment of bands as II−VI according to Jung et al. (1996a). For concentrations beyond 1 M KSCN,bands V and VI cannot be distinguished.

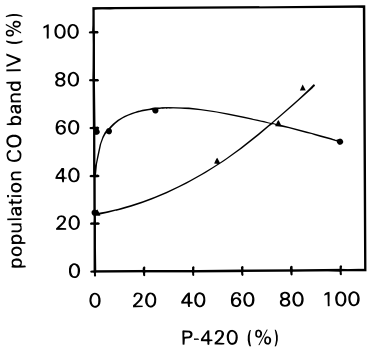

FIGURE 9: Correlation between the population of CO ligand subconformation IV with the cytochrome P-420 content for the thermal (●) and for the KSCN (▲) dependence studies.

structure alterations and P-420 formation. We found that, in both kinds of P-420 conversion, CO stretch band IV is predominantly affected. Thus, we plotted the population of this band versus the amount of P-420 formation (Figure 9). An increasing population of subconformation IV correlates almost linearly with an increasing formation of P-420 in the case of the KSCN-induced conversion. In contrast, for the thermally induced P-420, the population reaches a maximal value at a low P-420 content of approximately 25%, indicating that further protein unfolding leads to another subconformer equilibrium. The population increase of band IV is connected with a shift of this band to higher frequencies by up to 10 cm^{-1}.

CONCLUSIONS

For the first time, the Fourier transform infrared spectroscopy is applied to cytochrome P-450 to analyze the protein secondary structure. For substrate-free P-450cam, we estimate 44% α-helix, 31% β-sheet, and 18% turns. Camphor-bound P-450 shows a higher helix content of approximately 10%, resulting in 54% α-helix, 21% β-sheet, and 21% turns which agree with the crystallographic data of 53% α-helix, 19% β-sheet, and 16% turns. The good agreement between the percentage of secondary structure elements determined by this spectroscopic method and the values derived from the crystal structure gives us confidence in the applicability of FT-IR spectroscopy to the study of the P-450 to P-420 conversion. The present study clearly shows that the thermally induced P-420 formation is connected with the decrease of the α-helix content and the increase of the β-sheet population. We estimate for 100% P-420 obtained by thermal unfolding an α-helix content of 19%, a β-sheet content of 53%, and 14% turns. Additionally, 5−6% of the intermolecular antiparallel β-sheet structure is observed. Using KSCN, two types of inactivated forms of P-450 can be observed. Up to 1 M KSCN, inactivation occurs up to 77% without any big changes in the secondary structure of the protein, whereas with 1.5 M KSCN, the efficiency of the conversion is 85% but at the expense of more drastic variations of the overall structure of the cytochrome. At such a high concentration, KSCN may act as a salt in the Hofmeister's lyotropic series of ions which have a global effect on the protein structure (Imai & Sato, 1967). The observed decrease of the α-helix content and increase of the β-sheet character induced in the KSCN concentration range of 1−1.5 M is therefore connected with larger global changes similar to the alterations observed for the thermally induced P-420. This type of P-420 might be compatible with a histidine proximal ligand which has been detected for pressure-induced P-420cam−CO by resonance Raman measurements (Wells et al., 1992).

Below 1 M KSCN, the origin of the conversion to P-420 seems to be more complex. Binding of SCN^- to the heme iron in the oxidized state seems also to retain the thiolate ligand as shown by Sono et al. (1982) but might additionally destabilize the proximal thiolate ligand environment by facilitating a sulfur−iron stretching or a thiolate protonation after reduction and CO complex formation (Hanson et al., 1976; Jung, 1983, 1985). This would explain why no significant changes in the secondary structure appear while the stretch modes of the iron-bound CO ligand are blue shifted. Recently, Martinis et al. (1996) concluded from studies of the pressure-induced P-420cam formation using

different methods that in the ferric state the Cys357 is retained as the fifth iron ligand whereas it is protonated or lost after reduction and CO binding.

The present study using the stretching mode of the CO iron ligand shows also that the P-420 structure exists in an equilibrium of conformational substates as is observed for P-450. For P-450, we have argued that the different subconformers are caused by different packing of water molecules in the protein structure (Jung et al., 1996a,b) inducing a changed stretch mode frequency. In addition to this behavior, the possible change of the fifth ligand in P-420 does also induce frequency shifts which interfere with the effect of the different water packing. So further studies are necessary so we can differentiate between these two effects.

ACKNOWLEDGMENT

We are grateful to Dr. Otto Ristau for assistance in using his fit program.

REFERENCES

Arrondo, J. L. R., Young, N. M., & Mantsch, H. H. (1988) *Biochim. Biophys. Acta 952*, 261−268.

Banci, L., Bertini, I., Marconi, S., Pierattelli, R., & Sligar, S. G. (1994) *J. Am. Chem. Soc. 116*, 4866−4873.

Byler, D. M., & Susi, H. (1986) *Biopolymers 25*, 469−487.

Carrier, D., Mantsch, H. H., & Wong, P. T. T. (1990) *Biopolymers 29*, 837−844.

Champion, P. M., Gunsalus, I. C., & Wagner, G. C. (1978) *J. Am. Chem. Soc. 100*, 3744−3751.

Chirgadze, Yu. N., Fedorov, O. V., & Trushina, N. P. (1975) *Biopolymers 14*, 679−694.

Clark, A. H., Saunderson, D. H. P., & Suggett, A. (1981) *Int. J. Pept. Protein Res. 17*, 353−364.

Dawson, J. H., & Sono, M. (1987) *Chem. Rev. 87*, 1255−1276.

Dawson, J. H., Andersson, L. A., & Sono, M. (1992) *New J. Chem. 16*, 577−582.

Griffin, B. W., Peterson, J. A., & Estabrook, R. W. (1979) in *The Porphyrins* (Dolphin, D., Ed.), Vol. VII, pp 333−375, Academic Press, New York.

Gunsalus, I. C., & Sligar, S. G. (1978) *Adv. Enzymol. Relat. Areas Mol. Biol. 47*, 1−44.

Hanson, L. K., Eaton, W. A., Sligar, S. G., Gunsalus, I. C., Gouterman, M., & Connell, C. R. (1976) *J. Am. Chem. Soc. 98*, 2672−2674.

Harrington, W. F., & Hippel, P. H. (1961) *Arch. Biochem. Biophys. 92*, 100−112.

Holloway, P., & Mantsch, H. H. (1989) *Biochemistry 28*, 931−935.

Holzbaur, I. E., English, A. M., & Ismail, A. A.(1996) *Biochemistry 35*, 5488−5494.

Hui Bon Hoa, G., Di Primo, C., Dondaire, I., Sligar, S. G., Gunsalus, I. C., & Douzou, P. (1989) *Biochemistry 28*, 651−656.

Imai, Y., & Sato, R. (1967) *Eur. J. Biochem. 1*, 419−426.

Ismail, A. A., Mantsch, H. H., & Wong, P. T. T. (1992) *Biochim. Biophys. Acta 1121*, 183−188.

Jung, C. (1983) *Stud. Biophys. 93*, 225−230.

Jung, C. (1985) *Chem. Phys. Lett. 113* (6), 589−596.

Jung, C., & Marlow, F. (1987) *Stud. Biophys. 120* (3), 241−251.

Jung, C., Bendzko, P., Ristau, O., & Gunsalus, I. C. (1985) in *Cytochrome P450-Biochemistry and Induction* (Vereczky, L., & Magyar, K., Eds.) pp 19−22, Akademia Kiado, Budapest.

Jung, C., Hui Bon Hoa, G., Schröder, K. L., Simon, M., & Doucet, J. P. (1992) *Biochemistry 31*, 12855−12862.

Jung, C., Pfeil, W., Köpke, K., Schulze, H., & Ristau, O. (1994) in *Cytochrome P-450* (Lechner, M. C., Ed.) pp 543−546, John Libbey Eurotext, Paris.

Jung, C., Ristau, O., Schulze, H., & Sligar, S. G. (1996a) *Eur. J. Biochem. 235*, 660−669.

Jung, C., Schulze, H., & Deprez, E. (1996b) *Biochemistry 35*, 15088−15094.

Keller, R. M., Wüthrich, K., & Debrunner, G. P. (1972) *Proc. Natl. Acad. Sci. U.S.A. 69* (8) 2073−2075.

Krimm, S., & Bandekar, J. (1986) *Adv. Protein Chem. 38*, 181−364.

Li, T. L., Quillin, M. L., Phillips, G. N., Jr., & Olson, J. S. (1994) *Biochemistry 33*, 1433−1446.

Lipscomb, J. D. (1980) *Biochemistry 19*, 3590−3599.

Martinis, S. A., Blake, S. R., Hager, L. P., Sligar, S. G., Hui Bon Hoa, G., Rux, J. J., & Dawson, J. H. (1996) *Biochemistry 35*, 14530−14536.

Miyazawa, T. (1960) *J. Chem. Phys. 32*, 1647−1652.

Miyazawa, T., Shimanouchi, T., & Mizushima, S. (1956) *J. Chem. Phys. 24*, 408−418.

Muga, A., Surewicz, W. K., Wong, P. T. T., Mantsch, H. H., Vijay, K. S., & Shinohara, T. (1990) *Biochemistry 29*, 2925−2930.

Nelson, D. R., Kamatari, T., Waxman, D. J., Guengerich, F. P., Estabrook, R. W., Feyereisen, R., Gonzalez, F. J., Coon, M. J., Gunsalus, I. C., Gotoh, O., Okuda, K., & Nebert, D. W. (1993) *DNA Cell Biol. 12*, 1−51.

Nölting, B., Jung, C., & Snatzke, G. (1992) *Biochim. Biophys. Acta 1100*, 171−176.

O'Keefe, D. H., Ebel, R. E., Peterson, J. A., Maxwell, J. C., & Caughey, W. S. (1978) *Biochemistry 17*, 5845−5852.

Omura, T., & Sato, R. (1964) *J. Biol. Chem. 239*, 2370−2378.

Ortiz de Montellano, P. R. (1986) in *Cytochrome P-450—Structure, Mechanism, and Biochemistry* (Ortiz de Montellano, P. R., Ed.) Plenum Press, New York.

Ozaki, Y., Kitagawa, T., Kyogoku, Y., Imai, Y., Hashimoto-Yutsudo, C., & Sato, R. (1978) *Biochemistry 17*, 5826−5831.

Pfeil, W., Nölting, B. O., & Jung, C. (1993) *Biochemistry 32*, 8856−8862.

Philson, S. B., Debrunner, P. G., Schmidt, P. G., & Gunsalus, I. C. (1979) *J. Biol. Chem. 254*, 10173−10179.

Poulos, T. L., Perez, M., & Wagner, G. C. (1982) *J. Biol. Chem. 257*, 10427−10429.

Poulos, T. L., Finzel, B. C., & Howard, A. J. (1986) *Biochemistry 25*, 5314−5322.

Poulos, T. L., Finzel, B. C., & Howard, A. J. (1987) *J. Mol. Biol. 195*, 687−700.

Prestrelski, S. J., Byler, D. M., & Thompson, M. P. (1991) *Int. J. Pept. Protein Res. 37*, 508−512.

Rein, H., Jung, C., Ristsau, O., & Friedrich, J. (1984) in *Cytochrome P450* (Ruckpaul, K., & Rein, H., Eds.) pp 163−249, Akademie-Verlag, Berlin.

Scheidt, W. R., Lee, Y. J., Geiger, D. K., Taylor, K., & Hatano, K. (1982) *J. Am. Chem. Soc. 104*, 3367−3374.

Schenkman, J. B., & Greim, H. (1993) in *Handbook of Experimental Pharmacology*, Vol. 105, Springer-Verlag, Berlin.

Sligar, S. G., Filipovic, D., & Stayton, P. S. (1991) *Methods Enzymol. 206*, 31−49.

Sono, M., & Dawson, J. H. (1982) *J. Biol. Chem. 257*, 5496−5502.

Stern, J. O., Peisach, J., Blumberg, W. E., Lu, A. Y. H., & Levin, W. (1973) *Arch. Biochem. Biophys. 156*, 404−413.

Surewicz, W. K., & Mantsch, H. H. (1988) *Biochim. Biophys. Acta 952*, 115−130.

Susi, H., & Byler, D. M. (1986) *Methods Enzymol. 130*, 290−311.

Van Stokkum, I. H. M., Linsdell, H., Hadden, J. M., Haris, P. I., Chapman, D., & Bloemendal, M. (1995) *Biochemistry 34*, 10508−10518.

Wells, A. V., Li, P., Champion, P. M., Martinis, S. A., & Sligar, S. G. (1992) *Biochemistry 31*, 4384−4393.

White, R. E., & Coon, M. J. (1980) *Annu. Rev. Biochem. 49*, 315−356.

Wong, P. T. T. (1991) *Can. J. Chem. 69*, 1699−1704.

Yu, C. A., & Gunsalus, I. C. (1974) *J. Biol. Chem. 249*, 102−106.

BI9700173